Journal of Materials Research and Technology 40 (2026) 3496–3508

Contents lists available at ScienceDirect

Journal of Materials Research and Technology

journal homepage: www.elsevier.com/locate/jmrt

Evaluation of mechanical, thermal, and viscoelastic properties of polylactic-acid (PLA)/ banana peel powder (BPP) composite

Ahmad Irfan Nazarudin [a], Adi Azriff Basri [a,b,c,*], Ernnie Illyani Basri [a], Kamarul Arifin Ahmad [a,b], Mohammed Thariq Haji Hameed Sultan [a,c,d], Mohd Nor Faiz Norrahim [e], Mohd Rafein Zakaria [f]

[a] Department of Aerospace Engineering, Faculty of Engineering, Universiti Putra Malaysia, Serdang, Malaysia
[b] Aerospace Malaysian Research Center (AMRC), Universiti Putra Malaysia, Serdang, Malaysia
[c] Laboratory of Biocomposite Technology, Institute of Tropical Forestry and Forest Products (INTROP), Universiti Putra Malaysia, Serdang, Malaysia
[d] Aerospace Malaysia Innovation Centre (944751-A), Prime Minister's Department, ~MIGHT Partnership Hub, Cyberjaya, Malaysia
[e] Defence Research Institute, Universiti Pertahanan Nasional Malaysia, Kem Perdana Sungai Besi, 57000, Kuala Lumpur, Malaysia
[f] Department of Bioprocess Technology, Faculty of Biotechnology and Biomolecular Sciences, Universiti Putra Malaysia, 43400, Serdang, Selangor, Malaysia

ARTICLE INFO

Handling Editor: SN Monteiro

Keywords:
Dynamic mechanical analysis
PLA composite
Banana peel powder
Mechanical characterization
Polylactic acid

ABSTRACT

This research investigates the thermal, mechanical, and dynamic properties of PLA composites reinforced with banana peel powder (BPP). Composites with varying BPP contents were produced using melt blending followed by compression moulding. Mechanical testing, thermogravimetric analysis (TGA), and dynamic mechanical analysis (DMA) were conducted to evaluate performance. Thermal results highlight the influence of BPP filler content on heat transfer, thermal stability, and the viscoelastic behaviour of the PLA matrix. Morphological characteristics were examined through scanning electron microscopy (SEM) and visual inspection. PLA/BPP composites containing 1 wt%, achieved the highest flexural strength with 1.7x higher than pure PLA, while the 3 wt% composite exhibited the highest thermal resistance. One-way ANOVA test approved significant differences existed based on their increasing BPP wt% shown in F-values against F-critical. Despite being reduced relative to its pure counterpart, the 1 wt% PLA/BPP formulation also recorded the greatest storage and loss moduli. Conversely, an increase in BPP filler content is observed to significantly decrease the damping factor and its overall thermal stability. Agglomeration is shown in poor mechanical performance in 2 wt% and 3 wt% despite having high thermal resistance at temperature past 400 °C. This study significantly establishes systematic correlation between filler content and viscoelastic behaviour of PLA/BPP composites, identifying the optimal loading while explaining the degradation mechanisms through morphological analysis.

1. Introduction

In recent years, plastic wastes are generally increasing impactful towards the environment. These issues include global warming, pollution in various media of air, soil and water which in general most plastics can resist in harsh environments. Hence, their exceptional mechanical and thermal properties are known to induce this phenomena. In order to cope this issue, surging trend in research indicated a diversion from conventional petrochemical plastics into alternative compostable, more eco-friendly plastics. Polylactic Acid (PLA) is known to be one of the popular biopolymer which can be fabricated from corn starch, sugar beet, and other crops by fermentation. In addition, this polymer is known to exhibit biodegradation and acceptable mechanical properties, comparable to conventional plastics [1].

In Malaysia, crops of banana are produced annually in large quantities, with over 500,000 metric tons recorded in recent years, making it one of the top fruit commodities in the country [2]. This leads to substantial agricultural waste, with banana peels comprising approximately 30–40 % of the fruit's total weight. As a result, over 150,000 to 200,000 metric tons of banana peel waste is generated annually [3]. Improper disposal of this biodegradable waste can contribute to methane emissions, foul odour, and localized pollution, underscoring the need for sustainable waste valorization strategies such as its incorporation into biocomposites or bio-based materials. In addition, Saba banana is

* Corresponding author. Department of Aerospace Engineering, Faculty of Engineering, Universiti Putra Malaysia, Serdang, Malaysia.
E-mail address: adiazriff@upm.edu.my (A.A. Basri).

https://doi.org/10.1016/j.jmrt.2026.01.027
Received 26 August 2025; Received in revised form 26 November 2025; Accepted 5 January 2026
Available online 6 January 2026

known to exhibit high cellulose concentration compared to other banana species whereas studies found exceptional tensile modulus of 27 GPa [4]. Thermal properties of saba banana peel powder is known to be great as it can retain heat conductivity [5].

Polylactic acid (PLA), a biodegradable polymer derived from renewable sources, serves as a promising matrix for biocomposite development. When reinforced with natural fillers, PLA-based composites can enhance material performance while promoting circular economy practices. These includes kenaf-PLA, wood-PLA and banana fiber-PLA improved PLA's tensile up to 40 %, 20 % and 30 % respectively [6–8]. Though significant findings converges to banana filler which studies have shown that incorporating 5 wt% banana into PLA can improve flexural modulus by up to 60 % and enhance thermal resistance [4,9]. Commonly, fiber-based organic additives are popular for PLA composites as they can improve PLA's mechanical performance. Mechanical results has drastically proves that banana fiber has potential in developing improved PLA characteristics.

PLA composites are often exposed to dynamic conditions, where both load and temperature fluctuates whereas pure PLA struggles in exhibiting brittleness is specific temperatures. Thus, several researchers have investigated the performance of natural fiber-reinforced polymer composites under such dynamic loading conditions. Majhi et al. developed a Banana-PLA composite by mercerization in order to maximise cellulose content. Their study showed that the addition of the chemical treatment steps have enhanced the storage modulus and loss modulus of the PLA composite by 60 % and 8 % respectively. Hence, their findings indicating improved interfacial adhesion between distinct materials primarily causing improved stress transfer [10]. Komal et al. found that banana fiber reinforcement reduced the damping factor (Tan Δ), suggesting an improvement in the polymer's elastic properties. Fabrication method include extrusion compression moulding which they also concluded that fiber incorporation increased the glass transition temperature (T_g) of the composites [11]. Previous research has demonstrated that factors like the weaving pattern of the fiber mat and fiber loading significantly impact the dynamic behaviour of polymer composites. Interestingly, Venkateshwaran et al. reported that the use of a plain weave pattern in banana mat composites improved their dynamic mechanical properties [12]. From these studies, it can be inferred that countless studies for in dynamic mechanical analysis. Hence, fiber additive have more flexibility in their orientation in matrix and is more direct approach compared to filler-based additives. This shows studies for PLA-Filler are lacking especially in analysing their mechanical properties. Filler banana additives has the similar potential if proper fabrication method and tests are implemented to validate similar claims with fiber additives.

A very recent study on PLA/BPP composites which their mechanical properties are heavily discussed adjunct with thermal findings [5]. Though, research to date has not extensively explored the static and dynamic mechanical behaviour of green composites reinforced with promising Saba banana peel fillers. The current work aims to bridge this gap by systematically investigating the mechanical, thermal, and viscoelastic behaviours of PLA reinforced with varying banana peel powder (BPP) loadings (0.5–3 wt%). Specifically, this study seeks to evaluate the tensile and flexural performance of PLA/BPP composites to determine the optimal filler concentration, examine fracture morphology using SEM to relate with interfacial bonding and failure mechanisms. Hence, characterize the viscoelastic response through DMA results to assess the effects of BPP on stiffness and energy dissipation and analyze the thermal stability and transition behaviours using TGA and DSC to correlate thermal and mechanical properties. The outcomes are expected to identify the ideal composition for balanced mechanical strength and thermal performance, thereby supporting the development of sustainable, bio-based polymer composites with improved functionality.

2. Materials and methods

2.1. Materials

Saba banana wastes were collected from a store in Serdang, Malaysia. 3251D for injection grade of PLA was obtained from Innovative Precision Sdn Bhd. The specific gravity of supplied polymer was 1.24 g/cc' as per supplier specifications. Melting temperature (T_m) and glass transition temperature (T_g) of PLA were 150 °C–160 °C and 55 °C–60 °C respectively.

Images of banana peel powder were examined, as shown in Fig. 1. Sieved BPP has depicted more uniform particle sizes compared to unsieved BPP. Thus, sieving the powder is required to maintain the similar powder sizes as recent studies have indicated improved mechanical property compared to unsieved [13].

Fabricating a PLA/Banana Peel Powder (BPP) composite by repurposing peel waste into functional fillers, enhancing PLA's flexural strength by nearly twice. Through melt-blending and compression moulding, the material was shaped into single-use products. This offers an sustainable solution including everyday disposable items as waste are repurposed and current PLA mechanically improved.

2.2. Processing of BPP

Banana peels were separated from the waste, washed with probiotic soap to remove dirt, and isolated from the edible portion. The peels were then sliced into smaller pieces using a knife and scissors. Smaller sizes were prepared to optimize drying in an oven at 60 °C for 24 h. Once dried, the moisture-free peels were ground using a 400W high-powered blender (Panasonic, YG–SC–1589). The resulting powder was sieved using a 250 μm mesh. Grinding and sieving were repeated to obtain standardized banana peel particulates. Fig. 2 illustrates preparation of BPP accordingly from banana peel waste to powder.

2.3. Composite fabrication

Fig. 3 emphasizes step in composite PLA/BPP fabrication with Melt-Blend Mixer and Compression Moulding Machine.

2.3.1. Melt-blending of mixed material

The melt-blending process was carried out using a Brabender® Plastograph® EC internal mixer with a screw mechanism that simulates typical polymer extrusion. PLA pellets were added to the mixer running at 50 rotations per minute (RPM) and heated to 190 °C. Once fully melted, banana peel powder (BPP) was introduced and left for 15 min to ensure even dispersion. BPP was incorporated at weight fractions ranging from 0.5 wt% to 3 wt% in the PLA composite mixture.

2.3.2. Hot compression mould of hardened mixed mould

Fig. 3 shows that compression moulding machine model TECHNO-PRESS 40HC-B was used to fabricate the hardened composite plates. This equipment have pressure, cooling rate, total cycle time of 30 psi, 16 °C/min, and 15 min respectively. The blended material was crushed and layered between metal sheets with 3 mm thickness and OHP films before compression. The process involved an 8-min pre-heating stage, followed by a 5-min full press. A final cold pressing step for 5 min was applied to minimize voids and trapped air, preventing recrystallization. Total samples compositions are 5 in total, includes PLA, varying composites wt of 0.5 wt% BPP, 1 wt% BPP, 2 wt% BPP, and 3 wt% BPP renamed as Control, PLA/BPP/0.5, PLA/BPP/1, PLA/BPP/2 and PLA/BPP/3 respectively.

Fig. 1. Images of BPP (left), sieved BPP (right).

Fig. 2. Banana peel powder preparation.

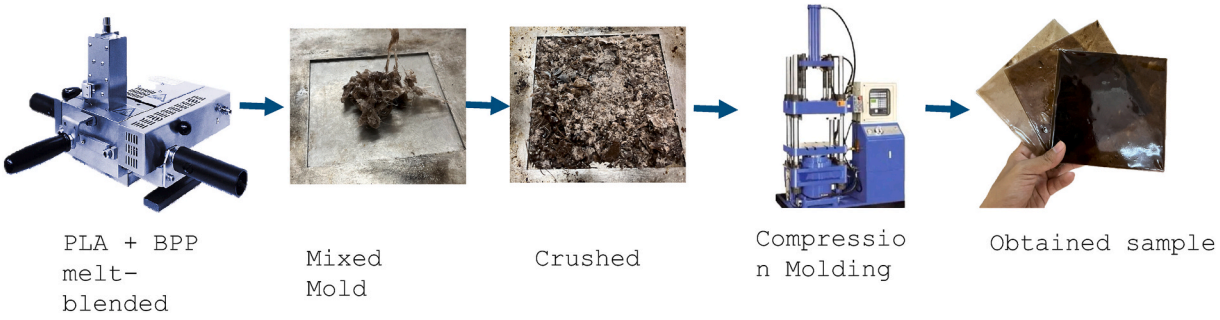

Fig. 3. Fabricating composite of PLA/BPP.

3. Characterisation

3.1. Tensile and flexural analysis

Physical testing was conducted using a Universal Testing Machine (INSTRON 5567) with appropriate load cells. Before testing, sample dimensions' thickness and length were measured using a micrometer screw gauge.

Tensile tests were carried out according to ASTM D638 using a 10 kN load cell, with a crosshead speed of 2.3 mm/min and strain rate between 1 and 500 mm/min. This standard prescribed dog-bone shaped dimensions of 115 mm (L) x 19 mm (W) x 3 mm (H). Flexural strength was assessed following ASTM D790-17 (Procedure A) using a wedge-action flexural clamp. Samples measured 120 mm × 12.7 mm and were tested with a 46 mm support span at a crosshead speed of 1.3 mm/min. A 50 kN load cell was used for the three-point bending tests.

3.2. Statistical analysis

The tensile, flexural, and impact strengths as well as the tensile and flexural modulus were each analyzed separately using an F-test in the form of a one-way (or one factor) analysis of variance (ANOVA) at a 5 % level of significance (95 % confidence level) to determine if the addition of the BPP had a statistical effect on the mechanical properties of the different composite groups. The only variable or factor changing was the filler loading. Each mechanical property was evaluated as one group which consisted of 5 groups where Group 1 was for pure PLA samples, Groups 2 to 5 for composites with increasing BPP loading from 0.5 %, 1 %, 2 % and 3 % BPP. The analysis was performed using the Analysis ToolPak add-in feature in Microsoft Excel 365 (Microsoft Corp., Redmond, WA, USA). If the F-critical value was less than the F-value, the results suggest significant differences of means exist between the composite groups (rejection of null hypothesis). If the F-value is close to zero or close to the F-critical value, it suggests there were no differences in the mean values obtained. If p-value is higher than 0.5, results can be deduced as statistically significant and not due to random chance, allowing to reject the null hypothesis.

3.3. Morphological analysis via scanning electron microscope (SEM)

Plate samples were initially examined using a digital camera before cutting. Tensile specimens containing varying fiber contents were analyzed using a scanning electron microscope (COXEM EM-30AX Plus, Korea). Cross-sectional imaging was performed at an accelerating voltage of 15.0 kV. To minimize image noise, all samples were gold-coated using a sputter coater prior to SEM analysis.

3.4. Thermal gravimetric analysis

Thermogravimetric Analysis (TGA) was conducted using a TGA analyzer (Mettler Toledo Model: TGA/DSC 3+ HT/1600) to evaluate the thermal stability and decomposition behaviour of the samples. Approximately 1–5 mg of each specimen was weighed and placed in a platinum pan. The analysis was performed under a nitrogen atmosphere to prevent oxidative degradation, with a continuous gas flow rate of 20–50 mL/min. The temperature range was set from room temperature to 600 °C, at a constant heating rate of 10 °C/min. The resulting TGA and derivative thermogravimetric (DTG) curves were recorded to identify the onset decomposition temperature (T_{onset}), peak decomposition temperature (T_{max}), and residual mass at 600 °C. This equipment specifically has DSC (Differential Scanning Calorimetry) function, but only the major peaks are discussed.

3.5. Melting crystallinity calculation

The degree of melting crystallinity (X_m) was determined using the following formula equation (1)

$$X_m = \frac{\Delta H_m}{(X_{PLA}\ \Delta H_m^o)}\ 100\% \quad (1)$$

ΔH_m represents the cold crystallization enthalpy of PLA/BPP composite; ΔH_m^o refers to the enthalpy value of 93.6 J/g for 100 % crystallized PLA [14]. X_{pla} defined as the weight fraction of PLA in the PLA/BPP composite.

3.6. Dynamic mechanical analysis

A Q800, TA Instruments DMA/SDTA equipped with dual cantilever tools was used for performing the DMA analysis. The test was run with a preload of 3 N and a frequency of 1 Hz. The samples were heated from 0 to 160 °C with at 3 °C/min in an air atmosphere. Based on ASTM D790, all samples were prepared as 60 x 12.5 × 3 mm^3.

4. Result and discussion

4.1. Tensile test

Fig. 4 emphasizes tensile properties including tensile strength, modulus and elongation at break of materials; PLA, PLA/BPP/0.5, PLA/BPP/1, PLA/BPP/2, PLA/BPP/3. All samples exhibited typical brittle fracture patterns. Neat PLA showed the highest mechanical performance, with tensile strength of 44.15 MPa, modulus of 5678.93 MPa, and elongation at break of 0.82 %, values comparable to conventional petroleum-based plastics. Upon incorporating banana peel (BPP) at 0.5 wt%, these values dropped to 39.47 MPa, 5915.81 MPa, and 0.74 % respectively. Increasing BPP to 1 wt% improved tensile properties, with strength reduce to 37.45 MPa, while increased its modulus to 5674.11 MPa, and elongation at break to 0.82 %. Hence, due to poor interfacial adhesion between the hydrophilic BPP and hydrophobic PLA will be proven in section 4.3. The mismatch in polarity limits stress transfer efficiency, leading to weak filler-matrix bonding and premature failure under load. Additionally, moisture affinity of BPP due to hydroxyl groups on its surface promotes micro-void formation and weakens the composite interface [15,16]. These interfacial defects hinder uniform stress distribution and reduce mechanical integrity. Similar trends have been reported in other particle-reinforced composites, where inadequate filler dispersion and particle size larger than 100 μm mesh reduce reinforcing efficiency [17]. However, achieving finer particle sizes requires higher energy input, theoretically making production less economical.

Followingly, reduced tensile properties is observed for BPP at 2 wt% where its strength (33.53 MPa) and elongation at break (0.61 %), while modulus is the highest of 6164.88 MPa. For this study, 3 wt% is the maximum BPP as the tensile properties is observed as the lowest including strength, modulus and elongation at break of 22.47 MPa, 5446.51 MPa and 0.44 % respectively. Contradicting values of increased young's modulus but decreased tensile strength verified in PLA/BPP/2 is experiencing more brittleness behaviour of PLA. As the stress is concentrated at poorly bonded filler interfaces, local debonding and crack propagation occur more readily, resulting in reduced tensile strength despite increased rigidity. This phenomenon is consistent with fracture mechanics principles, where higher stiffness without corresponding interfacial compatibility leads to reduced toughness and greater brittleness [18]. Additionally, consistent trend when compared for PLA/BPP/2 with PLA/BPP/3, overall tensile properties are reduced, as the loading increased. For instance, if the BPP loading is increased, expected tensile properties will be heavily reduced based on the pairing of result from these 2 loadings of PLA composites.

The tensile of the biocomposites are primarily influenced by the stretching of PLA molecular chains [19]. As BPP content increased from 0.5 wt% to 1 wt%, the interaction between PLA and BPP became more pronounced due to the higher number of polymer chains in contact with the filler. Hence, indicated from increase of elongation at break from 0.74 % to 0.82 % which has increased 10 % respect to 0.5 wt% BPP. Additionally, SEM analysis in a study confirmed that some BPP particulates penetrated the porous structure of, creating entangled regions that contributed to improved tensile deformation resistance [20]. However, when the BPP loading exceeded 2 wt%, the tensile properties began to decline. This reduction was attributed to poor dispersion and the formation of BPP agglomerates, which introduced stress concentration points within the matrix.

Overall of tensile test deduces that PLA/BPP/1 is the best composition for this study as their tensile properties experiencing the slightest deviations. Reduction of tensile stress compared to pure PLA, are only 15.17 %, and its young's modulus at only 0.08 %. Elongation at break values are found to be identical for this study.

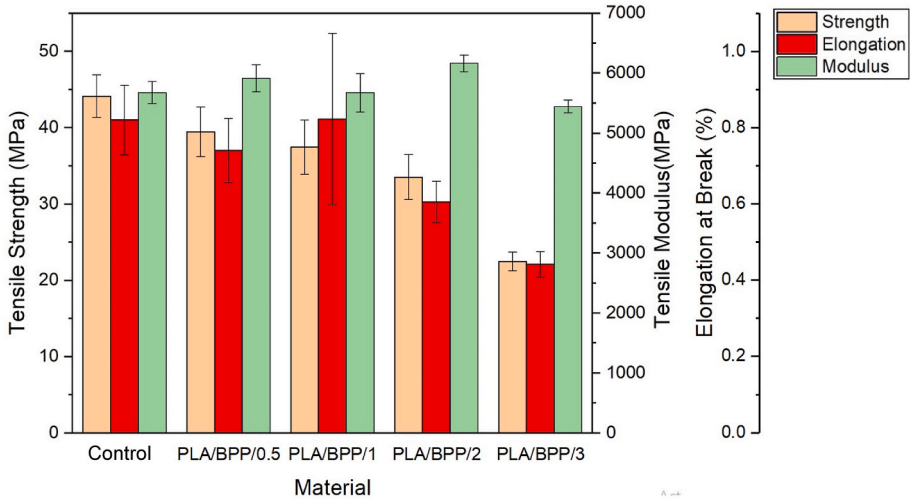

Fig. 4. Tensile properties of PLA and PLA-BPP composites.

4.2. Flexural test

Fig. 5 summarizes flexural properties including tensile strength, modulus and elongation at break for materials of PLA, PLA/BPP composites from 0.5 wt% to 3 wt%.

Neat PLA recorded flexural performance, with a strength of 40.76 MPa, modulus of 3037.22 MPa, and elongation at break of 1.75 %. When BPP of 0.5 wt% was added, these values slightly increased into 53.79 MPa, 3319.99 MPa, and 3.19 %, respectively. Followingly a modest addition to 1 wt%, increased these values into 70.51 MPa, 3504.78 MPa and 3.6 %. Though, inconsistent trend is observed for 2 wt%, as only modulus are increased to 3520.98 MPa while its strength and elongation at break depreciates to 25.38 MPa and 1.29 %. At 3 wt%, weakest flexural property is also observed which these values decreased to 13.67 MPa,3183.86 MPa and 1.38 %

In comparison with pure PLA, flexural strengths for PLA/BPP/0.5 is increased 31.96 %, followed by 72.99 % for PLA/BPP/1. Though, it decreases 37.74 % and 66.46 % for PLA/BPP/2 and PLA/BPP/3. Flexural modulus exhibited increase of 9.31 % for PLA/BPP/0.5, 15.39 % for PLA/BPP/1 followed by minute difference of 15.93 % for PLA/BPP/2. Similar trend of weakest mechanical property for PLA/BPP/3 which it reduces 12.22 %. Elongation at break results suggest increase of 82.19 % for PLA/BPP/0.5 followed by PLA/BPP/1. Though, for 3 wt% and 2 wt% shown only reduction of 21.14 % and 26.42 % respectively. This repeating trend from flexural properties is indicative of consistent increasing trend for flexural respect with increase of BPP loadings only from 0.5 wt% to 1 wt%. Though, this trend stops for when BPP loading exceeded 2 wt% and the flexural properties began to decline. Poor dispersion and the formation of BPP agglomerates is expected to be contributing this occurrence which inconsistent stress across the matrix.

In flexural results, presence of BPP within the PLA matrix have provided improved stress transfer induced better interfacial bonding in some regions by aiding the composite during bending test. As BPP content increased, the overall flexural modulus showed an increasing trend, peaking at 3520 MPa which is 15.93 % higher than pure PLA of only 3037.22 MPa. This enhancement may also be attributed to the interaction between PLA molecular chains and the porous structure of BPP, where partial chain entanglement or anchoring within the filler restricts mobility and provides greater resistance to bending deformation. The uniform dispersion of fillers during the preparation process contributed to the enhanced mechanical properties observed in the biocomposites compared to the neat PLA matrix. Notably, the use of untreated particulate reinforcements typically expected to promote cavitation and remains a point of interest. In particle-reinforced systems, the inherent stiffness and hardness of BPP made bending more difficult, often leading to stress concentration and microcrack initiation rather

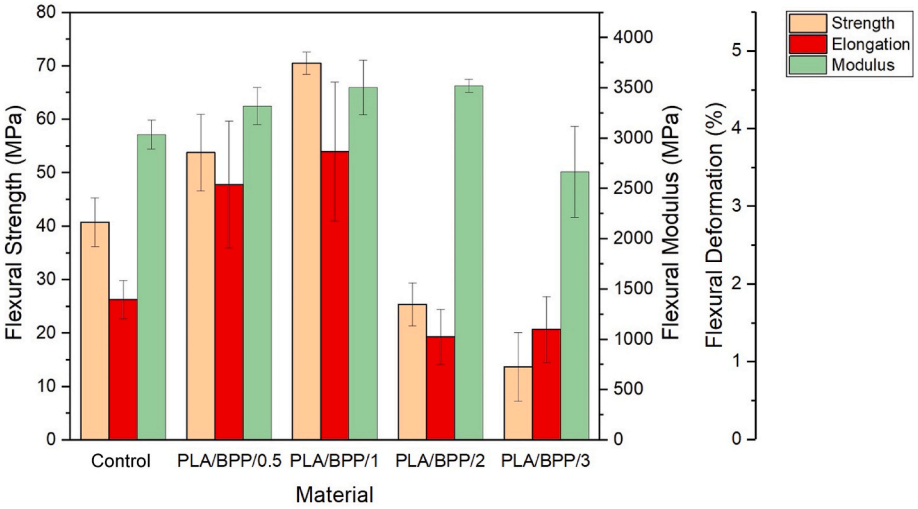

Fig. 5. Flexural properties of PLA and PLA-BPP composites.

than plastic deformation under flexural strain [21].

Similar findings were reported by Ho et al., who observed a 49.4 % increase in the total fracture energy of PLA composites when 7.5 wt% bamboo charcoal was added [22]. This improvement can be linked to the inherent properties of pure PLA, a semicrystalline polymer with limited crystallization ability and a relatively low degree of crystallinity, which results in poor resistance to impact. In other study, crystallization of BP and UFBC-reinforced biocomposites improved significantly, with crystallinity increasing alongside UFBC content. This enhancement allowed the molecular chains to self-organize into more regular structures, forming larger crystalline regions that improved resistance to the initiation of cracks [23].

4.3. Statistical analysis

Statistical evaluation using one-way ANOVA for tensile and flexural is summarized in Table 1. For all tests, the F-value exceeded the F-critical value, leading to rejection of the null hypothesis and confirming significant differences among the mechanical properties of the composites. The results indicate filler loading levels significantly influenced the tensile, flexural performance of the PLA matrix. Moreover, all test has shown P-values to be less than 0.05 and deduces that respective values among composites are statistically different.

F-values shown that flexural extension indicated the highest difference with F-critical value of 32.94 followed by tensile extension, flexural strength, tensile strength, flexural modulus and tensile modulus at 22.86, 22.81, 13.80, 2.76, 2.46 respectively. This values can deduce that extension for tensile and flexural results from section 4.2, shows the highest contribution. Similar studies has obtained f-values and implied that percentage contribution of the property can be proven with increased difference with f-critical value [24,25].

4.4. Scanning electron microscopy and morphology analysis

Scanning Electron Microscopy (SEM) analysis of fractured surfaces from composites with different filler loadings revealed distinct microstructural features corresponding to their mechanical properties. As shown in Fig. 6I and 6II, evident microcracks were present, indicating weak interfacial bonding and poor stress distribution. In other polymer-filler based composite study, SEM findings have indicated comparable behaviour with current morphology [26]. Similar pattern of grooves can be seen for the tensile tests sample across the 2 materials of PLA pure and PLA composite in Fig. 6. Due to its brittleness property, PLA is shown to be have apparent multiple matrix breakage with sizes ranges from 50 μm up to 59 μm where in this image observed total of 6 breakages.

Compared to PLA/BPP/1, number of breakage is reduced, despite being larger and differing sizes for each breakage points shown in high range values of 132 to 70 μm and total of 4 breakage in this image captured. Addition of BPP as filler-matrix interaction has provide strengthening effect as the number of breakage is reduced in the similar magnification. Visual interpretation of filler pull-out has indicated an apparent stress point compared to other breakages. Hence, fillers in PLA matrix has provide a degree of resistance through the PLA matrix. Though, due to the apparent sizes of the breakages are more apparent than pure PLA, has reflected into slight reduction peak tensile strength values as reported in section 4.1. Reducing the filler sizes and improving its surface adhesion for filler and matrix PLA may mitigate this issue as reported in other papers slight improvement in respective methods [27,28].

SEM images from Fig. 7(i) has indicated that BPP particles are relatively uniform distributed in PLA matrix surface. Particle sizes can be proven in scale provided where only 1–6 μm can be observed. This particle size measured complies with the sieving of BPP being less than 250 μm. This filler material property assessment is analogous with previous study on PLA composites [29]. Ideally, we can observe that Fig. 7(ii) emphasis on BPP uniform dispersion in PLA matrix in cross sectional area and be compared to isotropic figure of composite. This particle arrangement clarifies that BPP can provide strengthening effect by interlocking between PLA monomer chains as more contacts are provided. Hence, this will improve stress transfer across the matrix and might improve its mechanical performance. Apparently findings in section 4.2, has validated as the flexibility of PLA has improved drastically. Other studies has shown validation morphology analysis with increased mechanical strengths including PLA with rice husk and wood fillers [6,30].

Fig. 8(i) depicts visual breakage of cross-sectional surface respect with materials from pure PLA, PLA/BPP/0.5, PLA/BPP/1, PLA/BPP/2 and PLA/BPP/3. PLA shows the smoothest surface among the materials while other composites shown rougher surfaces. Meanwhile, significant voids is observed in PLA/BPP/2 cross-sectional surface of broken tensile samples. Followingly, PLA/BPP/3 show similar voids but with a significant size at the bottom part. Hence, void fraction is greater for composite 3 wt% relative to 2 wt%. Comparing to Fig. 8(ii), crack propagation for tensile test can induce cracks when the filler agglomerates. This can be relate with PLA/BPP/2 and PLA/BPP/3 as BPP agglomerates and instating more crack initiation sites across the matrix. This schematic also illustrates that occurrence of rougher surfaces on broken tensile samples as some BPP particles are left on the surfaces and missing post-tensile test. These defects facilitated crack initiation under tensile and flexural loading, with cracks propagating along the weak filler-matrix interface rather than through the matrix itself, indicating a brittle fracture mechanism. Similar findings can be observed for PLA with cellulose fillers experience agglomeration on higher filler loadings which the forces between the powder is stronger than the bond with the matrix [20,31].

4.5. Thermal characteristics

The TGA curves for all samples are illustrated in Fig. 9(i) and (ii), with key thermal degradation data summarized in Table 2. Pure PLA begins thermal degradation (T_{onset}) at approximately 259.98 °C, while composites containing BPP start slightly earlier, around 255.36 °C.

Table 1
ANOVA (One-way) was conducted to evaluate the effects of increasing BPP filler on tensile strength, tensile modulus, tensile elongation, flexural strength, flexural modulus, and flexural elongation of the PLA matrix.

Source of Variation	SS	df	MS	F-value	F-Critical	P-Value
Tensile Strength (MPa)						
BG	2081.34	4	520.33	16.66	2.87	3.732E-06
WG	624.59	20	31.23			
Tensile Modulus (GPa)						
BG	943.92	4	235.98	5.33	2.87	4.348E-03
WG	885.51	20	44.28			
Tensile Extension (%)						
BG	0.00	4	0.00	25.73	2.87	1.218E-07
WG	0.00	20	0.00			
Flexural Strength (MPa)						
BG	8892.70	4	2223.18	25.68	2.87	1.239E-07
WG	1731.58	20	86.58			
Flexural Modulus (GPa)						
BG	2118.87	4	529.72	5.63	2.87	3.350E-03
WG	1883.19	20	94.16			
Flexural Extension (%)						
BG	13.09	4	3.27	35.81	2.87	7.458E-09
WG	1.83	20	0.09			

(BG, between groups; WG, within groups; SS, sum of squares; df, degree of freedom; and MS, mean square).

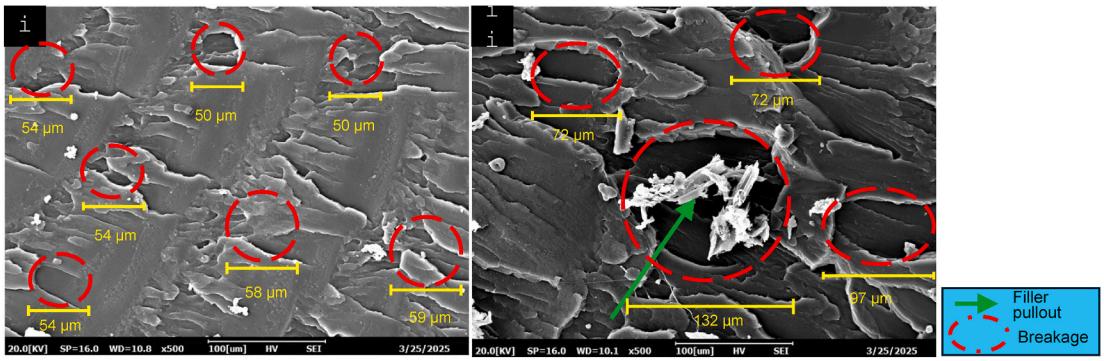

Fig. 6. SEM Images of surface area of broken tensile tests of PLA (i) and best performing PLA/BPP/1 (ii) (Enlargement at 500X).

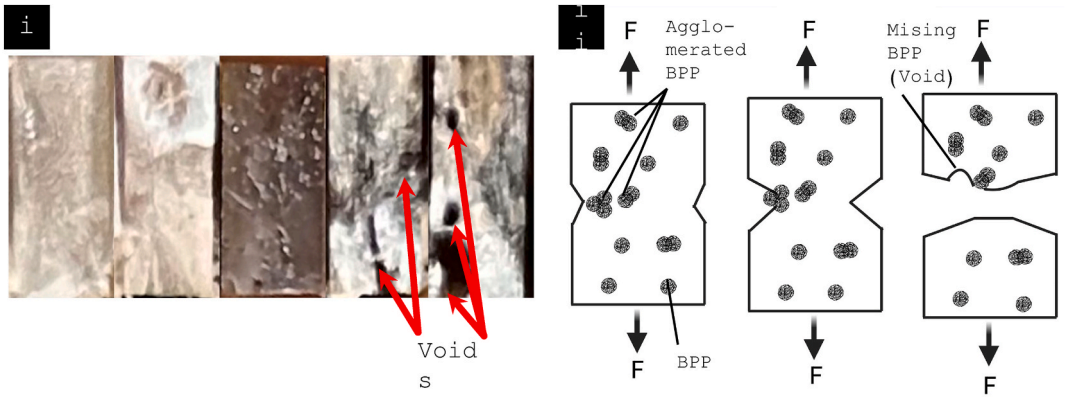

Fig. 7. Visual analysis of SEM images for depiction of powder dispersion in PLA matrix surface (ii) Schematic Illustration Isotropic arrangement of PLA-BPP matrix.

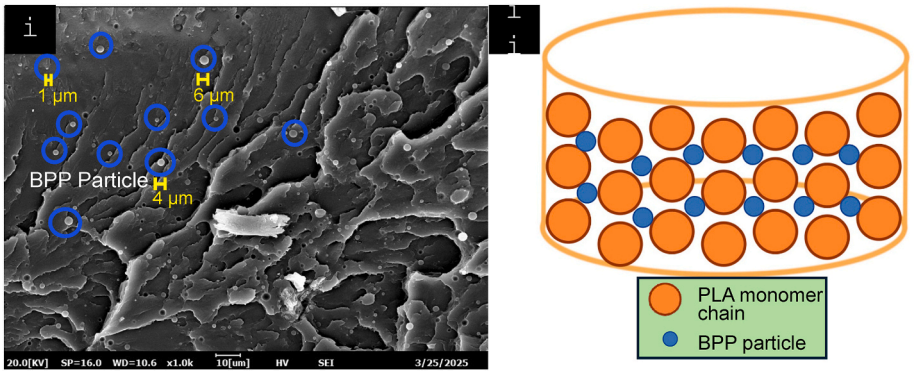

Fig. 8. (i) Cross sectional-area of breakage of Tensile Samples from left to right (PLA, PLA/BPP/0.5, PLA/BPP/1, PLA/BPP/2) and (ii) Schematic illustration of crack propagation for tensile breakage for agglomerated BPP in PLA matrix.

Among them, the 3 wt% BPP composite shows the lowest T_{onset}, likely due to the greater proportion of BPP, which exhibits lower thermal stability. The reduced T_{onset} across the composites suggests that increased filler incorporation may disrupt the polymer matrix and faster down gas release during thermal breakdown at lower temperatures. Hence, the TGA and DTG profiles show similar degradation trends across the samples. For 10 % mass residual, T_d shown 3 wt% has the lowest temperature, followed by 2 wt%, pure PLA, 1 wt% and 0.5 wt%. For decomposing temperature, PLA is improved only at lower loadings of 0.5 wt% and 1 wt% but worsens at higher loadings pass 2 wt%.

Interestingly at high temperatures, curve from the graphs depicts that decomposition continues up to about 400 °C for the 0.5 wt% and 1 wt% BPP composites, compared to roughly 380 °C for pure PLA, indicating the presence of additional degradable components in the blends. Followingly, 2 wt% and 3 wt% BPP composites complete degradation further than pure PLA, reflecting increased thermal resistance despite their weaker mechanical and morphological performance. At 10 % mass residuals, it can be observed that PLA/BPP/0.5 and PLA/BPP/1 exhibit increased temperature for 15.79 °C and 6.98 °C difference respectively compared to PLA. Conversely, higher loadings of 2 wt% and 3 wt% BPP shown reduced temperature with 10 % mass residual. Higher temperatures favors more on PLA/BPP composites of higher loadings as indicative of higher thermal retardancy. Hence, improved thermal stability can be found for PLA/BPP composite of lower loadings less than 1 wt% which is supported by its flexural properties found in Section 4.2. This aligns with earlier findings in polymer composite studies, where fillers contribute to higher residual mass upon degradation [23].

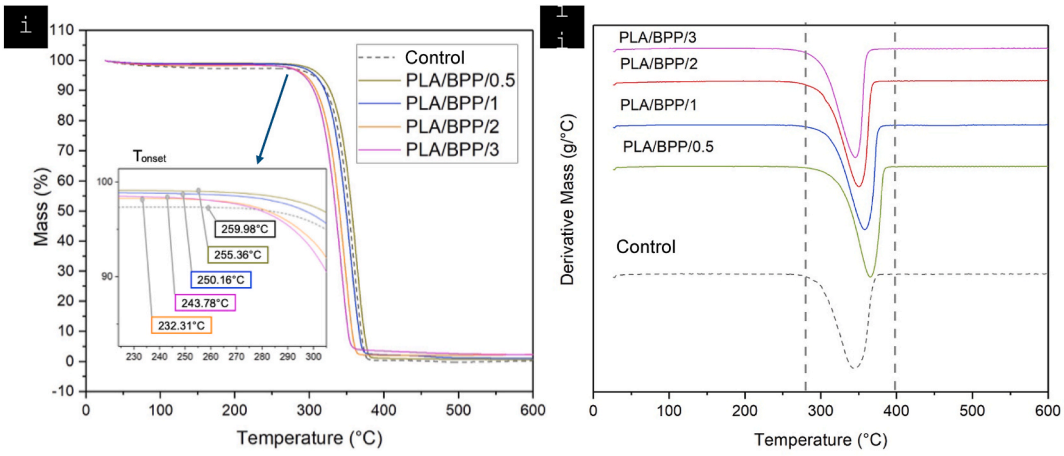

Fig. 9. (i) Thermal stability result based on decomposed mass.

Table 2
PLA and PLA/BPP composites with 10 % mass residual, respect with its T_d.

Material	Temperature, T_d (°C)
Control	359.479
PLA/BPP/0.5	373.26
PLA/BPP/1	366.397
PLA/BPP/2	356.826
PLA/BPP/3	351.789

4.6. Crystallization properties

In conjunction with previous study, FTIR findings have validated the compatibility of PLA and BPP which reflects to some composites with better crystallinity and interfacial adhesion that will be discuss here [5]. Table 3 summarizes the thermal parameters on melting point including glass transition temperature (T_g), degree of crystallinity (X_c) Melt crystallization temperature (T_m), initial border of melting phase (T_{m1}), final initial border for (T_{m2}), and melting crystallization enthalpy (ΔH_m). DSC data is obtained from recent study on PLA/BPP composites [32]. Several key trends emerge regarding the influence of BPP content on the thermal behaviour of PLA composites.

As the BPP content increased, the glass transition temperature (T_g) showed a moderate declining trend from 64.75 °C for pure PLA to 60.79 °C for the PLA/BPP/3 composite. This decrease in T_g may indicate a shift in the molecular mobility of the polymer chains under thermal conditions, suggesting a slightly earlier onset of thermal softening in higher BPP-loaded samples. More prominently, the degree of crystallinity (X_m) displayed a consistent increase with rising BPP content. Pure PLA registered an X_m of 32.23 %, while PLA/BPP/3 achieved the highest at 51.23 %, reflecting an overall enhancement in the ordered phase within the composite structure. This trend aligns with the melting enthalpy (ΔH_m) values, which rose from 30.17 J/g in neat PLA to 46.51 J/g in PLA/BPP/3, indicating a greater energy requirement for melting and, by extension, greater thermal stability of the crystalline regions.

Table 3
DSC data of PLA and PLA/BPP biocomposites.

Samples	T_g (°C)	X_c (%)	T_m (°C)	T_{m1} (°C)	T_{m2} (°C)	ΔH_m (J/g)
Control	64.75	32.23 %	171.46	154.61	182.02	30.1676703
PLA/BPP/0.5	63.91	44.21 %	167.98	149.34	180.54	41.1746475
PLA/BPP/1	64.57	42.14 %	168.28	149.45	183.2	39.047561
PLA/BPP/2	63.38	45.66 %	166.87	146.6	181.87	41.8817951
PLA/BPP/3	60.79	51.23 %	168.6	153.24	181.28	46.5115534

The melting temperature (T_m) values, though showing slight fluctuations, remained within a narrow range, with the highest T_m observed in the pure PLA at 171.46 °C, and the lowest at 166.87 °C in PLA/BPP/2. Interestingly, a rebound in T_m to 168.6 °C was recorded in the PLA/BPP/3 sample, indicating improved thermal uniformity at that loading. Dual melting temperatures (T_{m1} and T_{m2}) observed across all samples suggest the presence of complex melting behaviour, possibly due to multiple crystalline populations. T_{m1} values ranged from 146.60 °C to 154.61 °C, while T_{m2} values remained relatively stable between 180.54 °C and 183.20 °C, reflecting consistent high-temperature melting behaviour across samples. In conclusion, the PLA/BPP composites, particularly at 3 wt% BPP loading, demonstrate improved thermal performance as evidenced by higher crystallinity, elevated melting enthalpy, and stable melting temperatures. These enhancements point to improved heat resistance and thermal phase behaviour, making such composites more thermally robust than pure PLA.

At melting temperature, it can be inferred that increased BPP into PLA composite has concluded into higher enthalpy and crystallinity during melting temperature behaviour. Hence, BPP is known to exhibit high cellulose and silica content whereas exhibit high thermal resistance [4]. In addition, consecutive studies has proven heat and flame retardancy properties for banana peel powder [9]. In short, high melting crystallinity degree at PLA/BPP/3 which indicated 59 % better thermal characteristics than pure PLA has validated that BPP is a potent material in safety applications.

4.7. Dynamic mechanical analysis of PLA/BPP composite

In order to observe polymer-composite material's viscoelastic behaviour, dynamic mechanical analysis (DMA) is chosen as it is an established method. Cyclic-load (twisting) respect to temperature are analyzed which is time-independent deformation. Composition of materials can be easily identified for its viscoelastic behaviour, including results of storage Modulus (G′), loss modulus (G″) and damping factor (tan Δ). Respect with DMA method, mobility of polymer and their composites' molecules starts can be analyzed with its transition zone of composites. PLA is known to as a thermoplastic polymer, and can be defined into 4 graph regions; sub-glass transition (glassy) region, glass transition region, rubbery plateau and flowing region which will be discussed in respective sections. Fig. 10 emphasizes the general pattern of dynamic mechanical analysis of PLA as a thermoplastic [33].

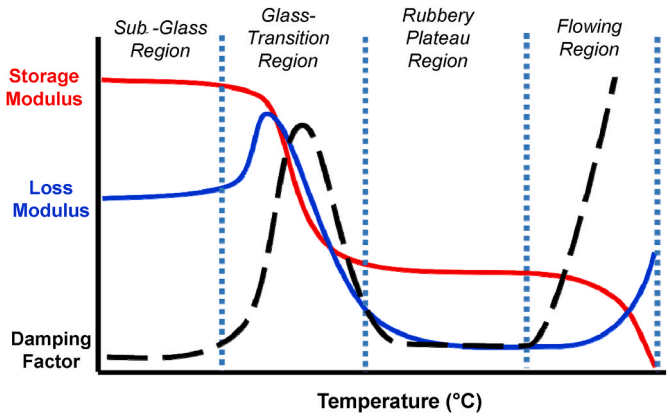

Fig. 10. A diagram illustrating the viscoelastic properties of a thermoplastic. (Adapted from Ref. [33]).

4.7.1. Storage modulus

The storage modulus represents the elastic or "stored" energy in a material when it is subjected to periodic deformation. It indicates the stiffness of the material and its ability to store mechanical energy. A higher storage modulus is typically associated with greater rigidity and resistance to deformation, reflecting a material's improved load-bearing capacity. In PLA-based composites, an increased storage modulus often results from strong filler-matrix interactions or crystalline structures, which enhance structural integrity and resistance to mechanical breakage under stress [33]. Fig. 11 summarizes PLA and PLA/BPP composites with relation of storage modulus respect to increasing temperature. Table 4 depicts the values of storage of modulus on specific temperature of T_{Room} (Room Temperature) and T_G (glass-transitioning temperature).

At room temperature, pure PLA exhibited the maximum storage modulus at 2050 MPa. In composite form, storage modulus of PLA/BPP/1 has reduced by 7.35 %, followed by PLA/BPP/0.5 (7.86 %), PLA/BPP/2 (~8 %) and PA/BPP/3 (9.26 %) (Refer Table 4). From this pattern, there is a direct correlation of particle concentration with decreasing storage modulus. Hence, in specific concentrations of BPP for 0.5 wt%, 2 wt%, 3 wt%, affects the chain mobility of PLA, which reduces the rigidity of PLA. Though in this study, PLA/BPP/1 having the least affected storage modulus at room temperature, is also supported with results from flexural stress tests whereas having the highest peak flexural stress, elongation at break values (refer Fig. 5).

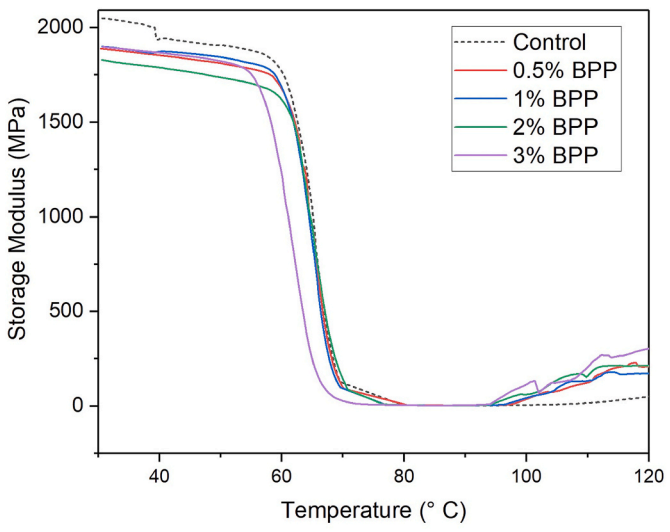

Fig. 11. Storage modulus of developed composites and PLA.

Table 4
Storage Modulus at Room Temperature vs Glass-Transition Temperature.

Material	Storage Modulus at T_{Room} (MPa)	Storage Modulus at T_G (MPa)
Control	2050.721	127.933
PLA/BPP/0.5	1889.631	91.711
PLA/BPP/1	1900.496	98.267
PLA/BPP/2	1830.728	85.267
PLA/BPP/3	1897.887	26.657

At glass-transitioning temperature, similar peak storage modulus is depicted by PLA which is 127.33 MPa. Minimum amount of BPP is added at 0.5 wt% and has resulted into reduced storage modulus at 91.71 MPa (28.31 %). Followingly, incremental BPP at 1 wt% added to PLA has resulted 98.27 MPa though less reduction relative to pure PLA of 23.19 %. PLA/BPP/2 and PLA/BPP/3 have following depreciated its storage modulus at 85.27 MPa and 26.66 MPa respectively. Massive reduction in storage modulus can be observed for PLA/BPP/3 is significant at 79.16 %, compared to PLA/BPP/2 at 33.35 %. This may be due to apparent voids and agglomeration (refer section 4.3 from SEM findings) occur on this particular BPP loadings as forces between particles are more apparent. Trends from the other studies, have shown reduced storage modulus at higher mass fractions due to this particular forces [34].

Compared to other developed composites, PLA/BPP/1 experience the least storage modulus reduction at 23.19 %. This sample also showed maximum flexural strength increase in earlier mechanical tests (refer section 4.2.Hence, this increase in PLA/BPP/1 confirms a toughening effect whereas the presence of BPP particles improved the composite's ability to resist deformation under dynamic mechanical stress. This particular composition verifies superior thermal-mechanical stability among the tested composites at glass transitioning temperatures. Recent findings indicated matching results, whereas the PLA-wood composites increases its mechanical properties while slightly reduced its storage modulus [35].

Fig. 11 emphasizes on the trend of storage modulus directly with rising temperature. Generally, from the very low temperature to high temperatures the behaviour of the polymer changes according to its molecular mobility. For PLA (control) room temperature up until 58 °C mark can be inferred as sub glass region indicates a small slope. Followingly, the storage modulus abruptly change and changes into very large gradient slope, can be inferred as glass-transition region. Rubbery region starts at 69 °C mark, as modulus reduces and stabilizes which the slope gradient reduced. In flowing region, modulus starts to increase at 100 °C but only exhibit small slope change. PLA 3251D is known to have high melting flow index and reflects to the high temperature of the flowing region [33,36].

Other composites of PLA/BPP share the similar curve profile with PLA of four regions. Though, slight deviation can be observed which point of the phase region transition occurs. Most significant difference can be observed for PLA/BPP/3 as sub glass region transition into glass region shifts at earlier at 54 °C mark. Next region also shifts the initial point at earlier temperature of 62 °C. Consistent shifting of lowered temperatures respect with region transitions can describe a reduced thermal stability and material stiffness. Hence, BPP at this mass-fraction induces worse particle energy dispersion towards the PLA matrix. This is also supported by the mechanical findings in section 4.1.

Similar to PLA, PLA/BPP/0.5 and PLA/BPP/1 indicate temperature, at 58 °C for glass region transitions into sub glass region. This is also reflected for the next region transition to rubbery also depicted at 69 °C. Unfortunately, the final region of rubbery transition shifts the temperature very early compared to PLA, at 95 °C in addition with higher gradient slope change. These two deviations exhibit worse molecular mobility and thermal stability at higher temperatures. Hence, BPP particles may disrupt the PLA matrix when in flowing form, as the viscosity is increased, though the stiffness is reduced.

In dynamic mechanical analysis (DMA), a steep gradient in the storage modulus curve during the glass transition phase signifies a rapid loss of stiffness, indicating that the material undergoes a sharp transition from a rigid to a flexible state. This steep decline reflects increased molecular mobility, where polymer chains gain freedom of movement, leading to a substantial reduction in mechanical resistance. In this study, for PLA showing such behaviour are more brittle, as less external force is required to initiate fracture once the glass transition is reached. Therefore, a high slope in the modulus-temperature curve corresponds to a less stiff and structurally unstable phase, making the material prone to deformation and breakage under minimal mechanical stress, especially at elevated temperatures. This property denotes a limited ability to retain load-bearing capabilities, highlighting the importance of a gradual modulus decline for improved toughness and durability in polymer composites. Conclusively, PLA/BPP/1 is known to exhibit the least affected storage modulus at T_{Room} and T_G, while increasing the BPP filler is known to be reducing the storage modulus. In fact, modern applications, PLA can only be use in room temperature applications including medical devices.

4.7.2. Loss modulus

The loss modulus quantifies the viscous or energy-dissipating component of the material during cyclic loading. It reflects how much mechanical energy is lost as heat. Materials with higher loss modulus values tend to exhibit better energy dissipation, which can be advantageous in damping applications [37]. In biocomposites, an increased loss modulus may indicate enhanced interfacial friction or mobility of molecular chains, often due to the presence of soft fillers or poor interfacial bonding [38].

The loss modulus results of PLA and PLA/BPP composites at varying filler loadings with respect to temperature are illustrated in Fig. 12. Incorporating banana peel powder (BPP) into neat PLA enhanced its loss modulus, reflecting improved interfacial energy dissipation. Among the developed composites, PLA/BPP/1 exhibited the highest peak loss modulus value of 405.76 MPa. PLA/BPP/2 achieved a peak value between PLA/BPP/1 and PLA/BPP/0.5, while PLA/BPP/3 recorded the lowest peak at 362.21 MPa.

Loss modulus indicates the amount of energy dissipated as heat under applied dynamic loading, which is strongly influenced by the adhesion quality between filler and matrix [39]. Materials with higher stiffness tend to dissipate more energy due to better stress transfer efficiency. As depicted in the figure, the loss modulus remains relatively constant at lower temperatures due to restricted mobility of PLA molecular chains. However, as the temperature increases, polymer chains gain mobility, resulting in a progressive rise in loss modulus values.

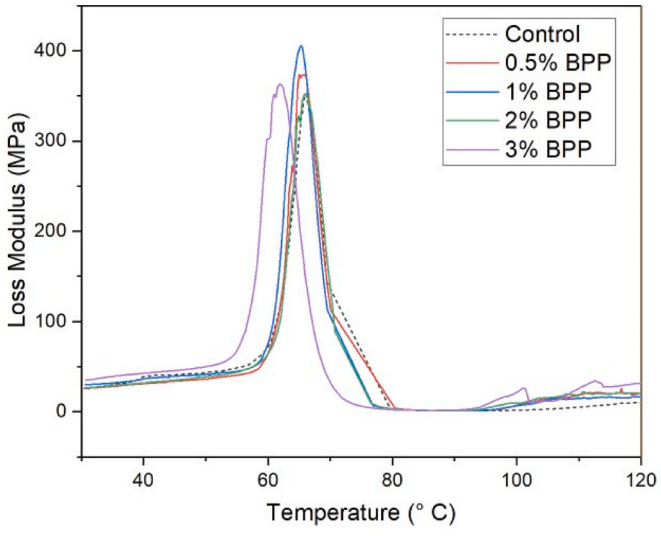

Fig. 12. Loss modulus of developed composites and PLA.

The variation in particle concentration and dispersion plays a critical role in dictating polymer chain movement and filler within the PLA/BPP composites. Particularly, PLA/BPP/1 showed superior filler-matrix interlocking as due to uniformly dispersed powder particles. This entanglement effect amplified interfacial friction, thereby enhancing energy dissipation under elevated temperatures and contributing to its highest loss modulus peak among the composites [40]. Conversely, the higher filler content in PLA/BPP/3 & PLA/BPP/2 lacks uniform dispersion and exhibit aggregation within BPP, reducing its interfacial bonding strength. The lack of structural interlocks in this composite led to interface weakening at higher temperatures, reflected in its lower loss modulus compared to composites with lower BPP content.

PLA/BPP/1 also retained the highest loss modulus at its glass transition temperature (65.29 °C), implying best dynamic stability under cyclic thermal and mechanical stresses among all composites produced. This result aligns with existing findings that emphasize the critical role of filler dispersion and interfacial adhesion in enhancing the energy dissipation characteristics of PLA-based biocomposites [41]. The detailed peak values and corresponding temperatures for each composite are summarized in Table 5. Recent findings indicated that increase of loss modulus at its glass transition relative to its pure polymer counterpart can indicate an improved energy dissipation capability and molecular chain mobility. This behavior reflects the material's greater ability to absorb and dissipate mechanical energy under dynamic loading, often associated with better stress relaxation, toughening effects, and reduced brittleness in the composite structure.

In short, the enhancement of loss modulus through banana peel powder (BPP) reinforcement highlights the potential of PLA/BPP composites for applications requiring improved energy dissipation and structural durability under dynamic loading. The PLA/BPP/1 composite, in particular, exhibited the highest peak loss modulus and maintained superior stability at elevated temperatures. Optimal filler dispersion and effective interfacial bonding ensured the composite's ability to absorb and dissipate mechanical energy, reducing the risk of premature failure in functional products. The observed trends outlines that peak loss modulus is greatly dependent on the BPP wt%, as it increased from Control followed with 0.5 wt%, peaks at 1 wt%. Though, specialized occurrences for composites past 2 wt%, as agglomeration happen, shown in sudden reduction in loss modulus. Hence, interface degradation occurs, compromising the composite's stiffness.

4.7.3. Damping factor

The damping factor, or tan Δ, is the direct ratio of the loss modulus to the storage modulus. It represents the material's ability to dissipate energy relative to its ability to store that energy. A higher tan Δ commonly indicates more viscous behaviour and greater damping, while a lower value suggests more elastic and rigid characteristics. In PLA composites, a lower tan δ is often linked with stiffer, more crystalline structures, while higher tan Δ may signal improved toughness or molecular mobility especially near the glass-transitioning temperature (T_G) [38]. Fig. 13 depicts the behaviour of damping factor correlate to rising temperature which Table 6 displays the damping factor for individual composites measured at their glass transition temperature.

Table 5
Loss modulus value of composites respective with temperature.

Materials	Peak of Loss Modulus G'' (MPa)	Temperature (°C)
Control	351.72	65.87
PLA/BPP/0.5	373.79	65.04
PLA/BPP/1	405.76	65.29
PLA/BPP/2	387.22	63.17
PLA/BPP/3	362.21	61.86

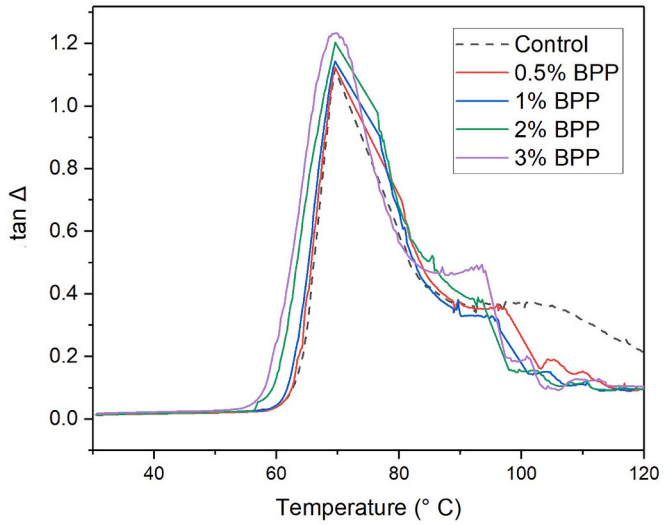

Fig. 13. Damping factor of developed composites and PLA.

Table 6
Damping factor and T_G, (glass-transitioning temperature) of PLA and its composites.

Composite Samples	Peak Temperature [T_G (°C)]	Damping Factor (Tan Δ)	T_G temperature difference towards pure PLA (°C)	Damping factor difference relative to pure PLA
Control	69.51	1.118	–	–
PLA/BPP/0.5	69.54	1.124	0.03	0.52 %
PLA/BPP/1	69.55	1.143	0.04	2.20 %
PLA/BPP/2	69.58	1.203	0.06	7.60 %
PLA/BPP/3	70.00	1.233	0.48	10.26 %

It can be observed that each material exhibit similar curve transition shape from initial of room temperature of 30 °C, up until 120 °C. Highest value of tan Δ is defined as the maximum damping factor while its temperature can be classed as T_G, (glass transitioning temperature).

The data reveals that incorporating BPP into PLA composites induces varying effects on the glass transition temperature (T_G) and damping factor (tan Δ) depending on the filler loading. At lower filler contents, specifically 0.5 wt% and 1 wt%, the T_G experiences a marginal increase of 0.03 °C and 0.04 °C, respectively, compared to neat PLA. This subtle rise suggests that small quantities of BPP have a negligible impact on the thermal softening behaviour of the polymer matrix. For filler content of 2 wt%, T_G increased by 0.06 °C is observed, indicating an increase in molecular mobility, possibly due to less effective filler-polymer interfacial adhesion that fails to restrict chain segment movements adequately. Interestingly, when the filler content is increased to 3 wt%, the T_G shifts upward by 0.48 °C, suggesting that at this loading, the BPP filler acts more effectively as a barrier to polymer chain motion, enhancing thermal stability.

Regarding the damping factor (tan Δ), a slight increment of 0.52 % and 2.20 % is noted for 0.5 wt% and 1 wt% BPP loadings, respectively. This indicates a minor increase in energy dissipation capacity through poor interfacial friction between the filler and matrix. Consequently 2 wt % BPP, the damping factor experiences a increase of 7.60 %, more than 3 times percentage difference relative to 1 wt%. Similarly at 3 wt%, there is significant increase in tan Δ by 10.26 %, highlighting pronounced energy dissipation through reduced internal friction as agglomeration may cause this issue. Hence, particle are more freely moving attributed to reduced stiffness but increased elasticity.

Overall, the trend demonstrates that at low BPP loadings of less than 1 wt%, the composite's thermo-mechanical behaviour remains relatively close to that of neat PLA shown less than 3 % damping factor difference despite slightly affecting the peak temperature. Nevertheless, high loading of BPP more than 2 wt%, have indicated greater reduction in damping factor which is more than 7 % difference relative to pure PLA. Hence, limits the material's ability to dissipate vibrational energy, thus reducing its potential for dynamic or impact-resistant applications. On the contrary, PLA/BPP/3, the composite exhibits enhanced thermal resistance and damping properties, signifying better stress absorption and molecular mobility restriction resulting from the increased filler-matrix interaction. Similar trend can be seen with other papers, which PLA incorporated with cellulose nanocrystals, which slight increasing T_G directly proportional with slightly increasing damping factor [42].

Another critical factor influencing the performance of binary biocomposites is the aggregate structure of PLA molecular chains. The heterogeneous mixture of PLA filler promote the formation of isotropic arrangement at the filler–matrix interface depicted in Fig. 7. Barrier properties of PLA and BPP may play a role as PLA-composite findings have reaffirm this phenomena directly affects these interactions [43]. These crystalline structures contribute to enhancing the modulus and strength of the biocomposites. This observation aligns with TGA analysis results, where increasing BPP content corresponds to higher crystallinity. Additionally, the PLA/BPP system behaves similarly to a matrix-aggregate composite, wherein BPP acts as the reinforcing framework and PLA provides the matrix strength. Under tensile loading, the mechanical performance predominantly depends on the interfacial adhesion between PLA and BPP, while under flexural loading, it is largely governed by the crystallization behaviour of the composite system.

5. Conclusion

This study demonstrated the feasibility of the incorporation of banana peel powder (BPP) into PLA matrix significantly influenced the mechanical and thermal performance of the developed biocomposites. PLA/BPP/1 composite exhibited the most effective mechanical behavior, achieving the highest flexural strength 1.7x higher than pure PLA and aggregation is verified at BPP past 2 wt%. This is supported by ANOVA results indicated that mechanical properties are statistically significant, particularly, flexural extension and tensile extension. At room temperature, DMA tests also this composite material shown highest storage modulus and loss modulus at 1900.4 MPa and 405.76 MPa. These findings suggest that the PLA/BPP composites can retain sufficient stiffness and elasticity for practical use in existing PLA applications include 3D printed implant based devices. TGA results revealed that while higher BPP content slightly reduced overall thermal stability at lower temperatures, the 2 wt% BPP composite showed enhanced resistance beyond 400 °C, suggesting potential for thermal retardant applications. Differential Scanning Calorimetry (DSC) results further confirmed the influence of filler loading on thermal transitions.

The present work effectively demonstrates a systematic correlation between filler content and the viscoelastic behavior of PLA/BPP composites, identifying the optimal filler loading while elucidating the underlying degradation mechanisms through morphological observations. Despite these promising outcomes, certain limitations remain as current study primarily focused on micro-scale BPP particles. Future work should incorporate nano-treated or surface-modified BPP fillers to improve filler–matrix compatibility and further enhance mechanical integrity. Additional investigations such as barrier property analysis, contact angle measurement, and X-ray diffraction (XRD) are recommended to understand the composites' interfacial characteristics and crystalline structure. Moreover, exploring the rheological and long-term degradation behaviors would provide deeper insights into processability and performance stability, thus advancing the development of high-performance, sustainable PLA-based composites.

Author contributions

Conceptualization: Adi Azriff, ; Methodology, Supervision, Project administration: Adi Azriff, Mohd Nor Faiz; Data collection and Analysis: Ahmad Irfan, Ernie Ilyani, Mohd Nor Faiz; Funding acquisition: Adi Azrif; Resources: Adi Azriff, Mohd Nor Faiz, Mohammed Thariq; Writing – original draft: Kamarul Ariffin Ahmad, Mohammad Thariq, Adi Azriff; Writing – review & editing: Ernie Ilyani, Mohd Rafein, Ahmad Irfan.

Declaration of competing interest

The authors declare the following financial interests/personal relationships which may be considered as potential competing interests: Adi Azriff bin Basri reports financial support was provided by Putra Malaysia University. If there are other authors, they declare that they have no known competing financial interests or personal relationships that could have appeared to influence the work reported in this paper.

Acknowledgment

The authors gratefully acknowledge the support provided by Universiti Putra Malaysia. This research was also funded by the Ministry of Higher Education, Malaysia through the Fundamental Research Grant Scheme (FRGS/1/2023/TK09/UPM/02/4).

References

[1] Hussain M, Khan SM, Shafiq M, Abbas N. A review on PLA-based biodegradable materials for biomedical applications. Giant Jun. 2024;18:100261. https://doi.org/10.1016/J.GIANT.2024.100261.
[2] Gobilik J, et al. Growth, yield and economic potential of cavendish banana planted in oil palm gaps [Online]. Available: http://tost.unise.org/; 2022.
[3] Vishala J, Singh G. A review on product development through pulp and peel OF banana. Plant Arch Jan. 2021;21(Suppliment-1):693–8. https://doi.org/10.51470/plantarchives.2021.v21.s1.104.
[4] Chaudhari CP, Bhole K, Gholave J. Review on Banana fibre-reinforced composites. Lecture Notes in Mechanical Engineering 2021:359–79. https://doi.org/10.1007/978-981-15-9117-4_27.
[5] Nazarudin AI, Basri AA, Basri EI, Ahmad KA, Haji Hameed Sultan MT, Tamagawa M. Thermal energy storage potential of Banana stem and peel: comparing heat conductivity at room temperature post-oven drying. Journal of Advanced Research Design Dec. 2024;123(1):23–33. https://doi.org/10.37934/ARD.123.1.2333.
[6] Zhang L, Lv S, Sun C, Wan L, Tan H, Zhang Y. Effect of MAH-g-PLA on the properties of wood fiber/polylactic acid composites. Polymers Nov. 2017;9(11):591. https://doi.org/10.3390/POLYM9110591. 2017, Vol. 9, Page 591.
[7] Mohamad M, Ting SW, Bakar MBA, Osman WHW. The effect of alkaline treatment on mechanical properties of polylactic acid reinforced with Kenaf Fiber Mat biocomposite. IOP Conf Ser Earth Environ Sci Dec. 2020;596(1):012002. https://doi.org/10.1088/1755-1315/596/1/012002.
[8] Chaitanya S, Singh I. Processing of PLA/sisal fiber biocomposites using direct- and extrusion-injection molding. Mater Manuf Process Apr. 2017;32(5):468–74. https://doi.org/10.1080/10426914.2016.1198034.
[9] Kong F, Nie B, Han C, Zhao D, Hou Y, Xu Y. Flame retardancy and thermal property of environment-friendly poly(lactic acid) composites based on Banana peel powder. Materials Aug. 2022;15(17):5977. https://doi.org/10.3390/MA15175977. 2022, Vol. 15, Page 5977.
[10] Majhi SK, Nayak SK, Mohanty S, Unnikrishnan L. Mechanical and fracture behavior of banana fiber reinforced polylactic acid biocomposites. International Journal of Plastics Technology 2010;14(1 SUPPL). https://doi.org/10.1007/s12588-010-0010-6.
[11] Komal UK, Lila MK, Singh I. PLA/banana fiber based sustainable biocomposites: a manufacturing perspective. Compos B Eng Jan. 2020;180:107535. https://doi.org/10.1016/J.COMPOSITESB.2019.107535.
[12] Venkateshwaran N, Elaya Perumal A, Arunsundaranayagam D. Fiber surface treatment and its effect on mechanical and visco-elastic behaviour of banana/epoxy composite. Mater Des 2013;47:151–9. https://doi.org/10.1016/J.MATDES.2012.12.001.
[13] Akindoyo JO, binti Husney NAA, Ismail NH, Mariatti M. Structure and performance of poly(lactic acid)/poly(butylene succinate-co-L-lactate) blend reinforced with rice husk and coconut shell filler. Polym Polym Compos Sep. 2021;29(7):992–1002. https://doi.org/10.1177/0967391120954047/ASSET/B154D498-132C-4018-8DB1-F105EED6ECDD/ASSETS/IMAGES/LARGE/10.1177_0967391120954047-FIG8.JPG.
[14] Al-Itry R, Lamnawar K, Maazouz A. Improvement of thermal stability, rheological and mechanical properties of PLA, PBAT and their blends by reactive extrusion with functionalized epoxy. Polym Degrad Stab Oct. 2012;97(10):1898–914. https://doi.org/10.1016/J.POLYMDEGRADSTAB.2012.06.028.
[15] Sanjay MR, Madhu P, Jawaid M, Senthamaraikannan P, Senthil S, Pradeep S. Characterization and properties of natural fiber polymer composites: a comprehensive review. J Clean Prod Jan. 2018;172:566–81. https://doi.org/10.1016/J.JCLEPRO.2017.10.101.
[16] Chen ZJ, et al. Barrier properties and hydrophobicity of biodegradable poly(lactic acid) composites reinforced with recycled Chinese spirits distiller's grains. Polymers Aug. 2021;13(17):2861. https://doi.org/10.3390/POLYM13172861. 2021, Vol. 13, Page 2861.
[17] Huang HX, Zhang JJ. Effects of filler–filler and polymer–filler interactions on rheological and mechanical properties of HDPE–Wood composites. J Appl Polym Sci Mar. 2009;111(6):2806–12. https://doi.org/10.1002/APP.29336.
[18] 'Atiqah Abdul Azam F, Tharazi I, Bakar Sulong A, Che Omar R, Muhamad N. Mechanical durability and degradation characteristics of long kenaf-reinforced PLA composites fabricated using an eco-friendly method. Eng Sci Technol Int J Sep. 2024;57:101820. https://doi.org/10.1016/J.JESTCH.2024.101820.
[19] Singh S, et al. Orientation of polylactic acid–chitin nanocomposite films via combined calendering and uniaxial drawing: effect on structure, mechanical, and thermal properties. Nanomaterials Dec. 2021;11(12):3308. https://doi.org/10.3390/NANO11123308/S1.
[20] Mouiya M, et al. Effect of sintering temperature on the microstructure and mechanical behavior of porous ceramics made from clay and banana peel powder. Results Mater Dec. 2019;4:100028. https://doi.org/10.1016/J.RINMA.2019.100028.
[21] Chandran AJ, Rangappa SM, Suyambulingam I, Siengchin S. Micro/nano fillers for value-added polymer composites: a comprehensive review. J Vinyl Addit Technol Sep. 2024;30(5):1083–123. https://doi.org/10.1002/VNL.22106.
[22] Ho MP, Lau KT, Wang H, Hui D. Improvement on the properties of polylactic acid (PLA) using bamboo charcoal particles. Compos B Eng Jul. 2015;81:14–25. https://doi.org/10.1016/J.COMPOSITESB.2015.05.048.
[23] Qian S, Tao Y, Ruan Y, Fontanillo Lopez CA, Xu L. Ultrafine bamboo-char as a new reinforcement in poly(lactic acid)/bamboo particle biocomposites: the effects on mechanical, thermal, and morphological properties. J Mater Res Nov. 2018;33(22):3870–9. https://doi.org/10.1557/JMR.2018.290.
[24] Benzannache N, Bezazi A, Bouchelaghem H, Boumaaza M, Amziane S, Scarpa F. Statistical analysis of 3-Point bending properties of polymer concretes made from marble powder waste, sand grains, and polyester resin. Mech Compos Mater Jan. 2018;53(6):781–90. https://doi.org/10.1007/s11029-018-9703-2.
[25] Ismail NAN, et al. Mechanical properties of novel hybrid bamboo Fibre/aluminium mesh reinforced polymer composite. Pertanika J Sci Technol 2024;32(Sp5):1–19. https://doi.org/10.47836/PJST.32.S5.01.
[26] Tsou CH, et al. Enhanced performance of nanoplate-carbon nanotube reinforced poly(butylene succinate) nanocomposites for sustainable packaging and multifunctional applications. Food Chem X Oct. 2025;31:102989. https://doi.org/10.1016/J.FOCHX.2025.102989.
[27] Tran TPT, Bénézet JC, Bergeret A. Rice and einkorn wheat husks reinforced poly (lactic acid) (PLA) biocomposites: effects of alkaline and silane surface treatments of husks. Ind Crops Prod Jul. 2014;58:111–24. https://doi.org/10.1016/J.INDCROP.2014.04.012.
[28] Miller K, Reichert CL, Loeffler M, Schmid M. Effect of particle size on the physical properties of PLA/potato peel composites. Compounds Mar. 2024;4(1):119–40. https://doi.org/10.3390/COMPOUNDS4010006/S1.
[29] Tsou CH, et al. High-performance conductive nanocomposites of modified poly (lactic acid) and nanocarbon Black: enhanced mechanical properties, chemically proven 3D network structure, and antibacterial features for 3D printing. Int J Biol Macromol Sep. 2025;322:146683. https://doi.org/10.1016/J.IJBIOMAC.2025.146683.
[30] Vengadesan E, Morakul S, Muralidharan S, Pullela PK, Alarifi A, Arunkumar T. Enhancement of polylactic acid (PLA) with hybrid biomass-derived rice husk and biocarbon fillers: a comprehensive experimental study. Discov Appl Sci Mar. 2025;7(3):1–24. https://doi.org/10.1007/S42452-025-06583-4/FIGURES/17.
[31] Kothavade PA, Shanmuganathan K. Mechanical properties of PLA/nanocellulose composites. Polylactic Acid-Based Nanocellulose and Cellulose Composites Mar. 2022:181–206. https://doi.org/10.1201/9781003160458-9.
[32] Nazarudin AI, et al. Mechanical and thermal performance of polylactic acid (PLA)-Saba banana peel composite. J Mater Res Technol Sep. 2025;38:1552–62. https://doi.org/10.1016/J.JMRT.2025.07.280.
[33] Cristea M, Ionita D, Iftime MM. Dynamic mechanical analysis investigations of PLA-based renewable materials: how are they useful? Materials Nov. 2020;13(22):5302. https://doi.org/10.3390/MA13225302. 2020, Vol. 13, Page 5302.
[34] Orisekeh DK, Corti G, Jahan MP. Enhancing thermo-mechanical properties of additively manufactured PLA using eggshell microparticle fillers. J Manuf Process Jan. 2025;133:782–97. https://doi.org/10.1016/J.JMAPRO.2024.11.095.
[35] Krapež Tomec D, Schöflinger M, Leßlhumer J, Žigon J, Humar M, Kariž M. Effect of thermal modification of wood on the rheology, mechanical properties and dimensional stability of wood composite filaments and 3D-printed parts. Wood Mater Sci Eng Nov. 2024;19(6):1251–65. https://doi.org/10.1080/17480272.2024.2316740.
[36] Khan I, kumar Neeraj, Yadav JS, Choudhary M, Chauhan A, Singh T. Utilization of waste slate powder in poly(lactic acid) based composite for 3D printer filament. J Mater Res Technol May 2023;24:703–14. https://doi.org/10.1016/J.JMRT.2023.03.046.
[37] Johari MAF, et al. The effect of microparticles on the storage modulus and durability behavior of magnetorheological elastomer. Micromachines Aug. 2021;12(8):948. https://doi.org/10.3390/MI12080948. 2021, Vol. 12, Page 948.
[38] Chaudhary V, Dwivedi SP, Das PP, Gupta P, Sharma B. An investigation of fatigue, creep, and dynamic mechanical behavior of bio-fiber-reinforced PLA and their

hybrid biocomposites. Biomass Convers Biorefin Mar. 2025;15(5):7623–33. https://doi.org/10.1007/S13399-024-05629-8/METRICS.

[39] Guo J, Chen X, Wang J, He Y, Xie H, Zheng Q. The influence of compatibility on the structure and properties of PLA/lignin biocomposites by chemical modification. Polymers Jan. 2019;12(1):56. https://doi.org/10.3390/POLYM12010056.

[40] Tandon GP, Pochiraju K. Environmental durability of polymer matrix composites. Comprehensive Composite Materials Jan. 2017;II:131–58. https://doi.org/10.1016/B978-0-12-803581-8.10044-X.

[41] Manral A, Ahmad F, Chaudhary V. Static and dynamic mechanical properties of PLA bio-composite with hybrid reinforcement of flax and jute. Mater Today Proc Jan. 2020;25:577–80. https://doi.org/10.1016/J.MATPR.2019.07.240.

[42] Agbakoba VC, Hlangothi P, Andrew J, John MJ. Mechanical and shape memory properties of 3D-Printed cellulose nanocrystal (CNC)-reinforced polylactic acid bionanocomposites for potential 4D applications. Sustainability Oct. 2022;14(19):12759. https://doi.org/10.3390/SU141912759. 2022, Vol. 14, Page 12759.

[43] Guo J, et al. Preparation and characterization of bio-based green renewable composites from poly(lactic acid) reinforced with corn stover. J Polym Res Jun. 2021;28(6). https://doi.org/10.1007/s10965-021-02559-1.